neel.cnrs.fr

Highlights 2015

NÉEL institut

Editorial

The Institut NÉEL, Grenoble, is a laboratory of the CNRS devoted principally to basic research in condensed-matter physics, enriched by interdisciplinary activities at the interfaces with chemistry, engineering and biology. With a total of 450 staff including more than 100 PhD students, it is one of the largest physics laboratories in France. Our major research fields are:

- Magnetism and spintronics,
- Photonics, plasmonics and non-linear optics,
- Correlated systems, quantum fluids and superconductivity,
- Quantum, molecular and wide bandgap electronics,
- Materials: their synthesis, structure and functions,
- Instrumentation.

These interlinked domains are developed across our three scientific departments, which are constituted from a total of 17 research teams supported by a similar number of transverse technology teams and services.

This 2015 issue of the Institute's "*Highlights*" magazine contains sixteen short articles specially written to describe particularly important scientific or technical advances made recently in our laboratory. This is of course far from being an exhaustive list, and a much more complete overview of our activities can be found at our website www.neel.cnrs.fr, together with pdf versions of all previous issues of the "*Highlights*" magazine.

The present issue also features an article describing our visitors' centre, the "PHYSIQUARIUM", which was created for an audience wider than this magazine's readership. It offers a pedagogical presentation of our laboratory's research subjects and provides the opportunity for visitors to perform simple experiments. Opened in 2014, it now attracts a large number of high-school classes and other visitors.

The year 2016 will bring considerable changes for the Institut NÉEL, at two levels. At the internal level, a new team of directors will take over from the team formerly led by Alain Schuhl and at present by myself. At another level, three of Grenoble's universities will be amalgamated in 2016 to create the pluridisciplinary Université Grenoble Alpes, and a "Communauté Université Grenoble Alpes" will coordinate university, engineering school and public laboratory research across the Grenoble and Alpine area. Thus, new collective challenges of great importance are ahead of us, which will make this new year (and following years) additionally stimulating for Institut NÉEL staff.

I wish you interesting reading in this 2015 issue of our *Highlights* magazine.

Hervé COURTOIS
Director of Institut NÉEL
Grenoble, France

Contents

DIRECTOR OF PUBLICATION
Hervé COURTOIS

EDITORS
Signe SEIDELIN, Jan VOGEL, Ronald COX

PRODUCTION MANAGER
Nathalie BOURGEAT-LAMI

LAYOUT
Élodie BERNARD
Florence FERNANDEZ

PRINTING
Press'Vercors
November 2015

Measuring the phase shift of an electron scattered by a single spin

Quantum interference is one of the most mysterious features of quantum mechanics. A well-known example is the Young double-slit experiment which demonstrates that light can be described at the same time by a particle picture and by a wave picture – the famous particle-wave duality. The same can be said of electrons when they pass through a two-path interferometer. In this article, we show that an electron interferometer can be used to measure a very intriguing effect postulated to arise when electrons are scattered off a magnetic impurity at temperatures near the zero temperature limit. In this case the electrons should acquire a phase shift of $\pi/2$, contrary to what is observed when an electron scatters off a static impurity. This phase shift, predicted as early as 1974 has finally been measured using a micron scale, quantum interferometer.

The electrical resistance of a pure metal usually drops when the temperature is lowered because electrons can travel through the crystal more easily when lattice vibrations are reduced. However below a temperature of approximately 10 K the resistance stops falling, stabilising at a level determined by scattering by lattice defects in the material. Upon further cooling, some metals – for example lead or aluminium – can suddenly lose their electrical resistance and become super-conducting, but "normal" metals, like copper, silver or gold do not show superconductivity and have a finite resistance even at the lowest accessible temperatures.

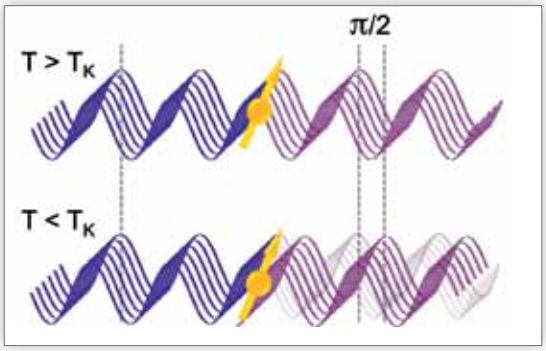

Fig. 1: *Phase shift across a Kondo "impurity": a foreign atom or a localised electron. Above a characteristic temperature T_K associated with the Kondo effect the incident electron wave is scattered without any phase shift. Below this temperature, a $\pi/2$ phase shift due to the Kondo effect has been observed for the first time in this work.*

When normal metals contain a tiny amount of magnetic impurities, such as iron or cobalt, they show a different, very unusual behaviour. In this case the electrical resistance does not stay constant when the temperature approaches absolute zero, but it increases. This effect puzzled physicists over many decades and it became known as the Kondo effect, after the Japanese physicist Jun Kondo who was the first to give an explanation of the unusual resistance increase in 1964.

Electrons carry not only an electric charge but also a magnetic moment associated with their spin. The interaction of this magnetic moment with magnetic impurities generates collisions of a novel type, which become more and more efficient as the temperature is lowered. The result of these interactions is the formation of a large static cloud of electrons, often called the Kondo cloud. At very low temperatures (well below 1 deg. K), this cloud of electron spins screens the magnetic impurity and acts like a large, static "impurity", scattering other electrons passing nearby. This is the Kondo effect.

It is believed that, when an electron is scattered by the Kondo cloud, the electron's wave function acquires a phase shift of $\pi/2$ (see Fig.1) as predicted by the French physicist Philippe Nozières in 1974. This predicted phase shift, however, has stayed elusive for 40 years. This is because one has to be able to isolate a *single* magnetic impurity to demonstrate the effect. That requires sophisticated nanofabrication techniques that have only become available in the last decade. In addition, in order to detect the phase shift, phase sensitive measurements similar to the Young double slit experiment have to be realized for a system of electrons.

A single localized electron can scatter mobile electrons exactly like a single magnetic impurity, and it can be controlled more easily than an impurity atom. A single electron can now be trapped routinely within a sub-micron electrostatic trap, called a "quantum dot", defined in a two-dimensional electron gas by carefully shaped electrodes. In this device, a Kondo cloud will form in the surrounding electron gas.

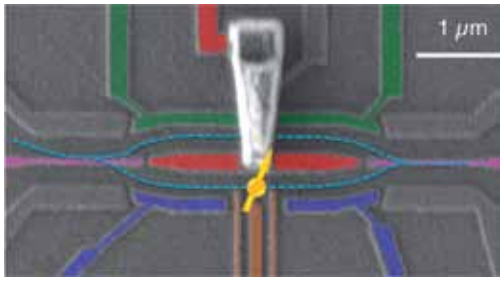

Fig. 2: *Quantum interferometer made by depositing electrostatic gates onto a two-dimensional electron gas in a semiconductor device. The blue dotted lines depict the two possible paths for electrons passing through the interferometer. A quantum dot containing a single localised electronic spin (in yellow), which acts as an effective Kondo "impurity", is inserted in one of the arms of the interferometer.*

By inserting such a quantum dot in one arm of a quantum interferometer (Fig. 2), we have been able to measure the predicted $\pi/2$ phase shift (Fig. 1) in the regime of the Kondo scattering, which sets in at temperatures of the order of one hundredth of a degree Kelvin for this system.

Using powerful computing algorithms to compare our measurements with exact numerical results of modern theory, we have shown that this scenario, based on the Kondo effect, is correct. The understanding of electrical transport in metals has thus reached a new level: the most modern theoretical models appear to be essential for a complete comprehension of phenomena as basic as the electronic transport governing the resistance of metals.

CONTACT

Christopher BÄUERLE
christopher.bauerle@neel.cnrs.fr

Tristan MEUNIER
tristan.meunier@neel.cnrs.fr

Ph.D student:
Shintaro TAKADA

FURTHER READING

"Transmission phase in the Kondo regime revealed in a true two-path interferometer"

S. Takada, C. Bäuerle, M. Yamamoto, K. Watanabe, S. Hermelin, T. Meunier, A. Alex, A. Weichselbaum, J. von Delft, A. D. Wieck and S. Tarucha

Phys. Rev. Lett. 113, 126601 (2014).

"Measurement of the Transmission Phase of an Electron in a Quantum Two-Path Interferometer"

S. Takada, M. Yamamoto, C. Bäuerle, K. Watanabe, A. Ludwig, A. D. Wieck and S. Tarucha

Appl. Phys. Lett. 107, 063101 (2015).

Imaging interfaces in artificial semiconductor crystals

Many electronic and optoelectronic devices are fabricated from semiconducting "superlattices": a sequence of alternating, thin layers of two different semiconducting compounds that have the same crystal structure. A superlattice is like a single crystal, but one that has periodic, abrupt changes of composition at the interfaces between its two constituent compounds. Usually these are compounds of a metal and a nonmetal where only the metal component is modulated (*e.g.* Gallium Arsenide/ Aluminium Arsenide superlattices, a classic example). We have been studying the interesting case of superlattices where both the metal atoms (the cations) and the non-metal atoms (the anions) are different in the alternate layers. The atomic configurations at the interfaces between two layers is then intrinsically complex, but can be unravelled by ultra-high resolution electron microscopy.

Superlattices built from two compounds with no atom in common exhibit special optical and electronic properties. We have been investigating Zinc Telluride / Cadmium Selenide (ZnTe/CdSe) short-period superlattices, as potentially efficient absorbers of sunlight for solar cells. Our superlattices are alternating thin layers of ZnTe and CdSe with repeat period of order 10 nm. They are grown by Molecular Beam Epitaxy (MBE), the technique of choice to realize semiconductor hetero-structures with flat, sharp interfaces. In this context a precise knowledge of the interfaces is crucial for "engineering" the optical absorption threshold: The short period makes the optical absorption properties very sensitive to the atomic arrangement at the interface.

To take the simplest possibilities, at the interface, do we have Zn atoms bound to Se, or Cd atoms bound to Te? Or more complex configurations? To answer these questions, we used a state-of-the-art Transmission Electron Microscope, located at the Nano-Characterization Platform (PFNC) at CEA-Minatec (Grenoble), whose resolution has been enhanced to better than 0.1 nm by correcting magnetic-lens aberrations. We used a mode where the image contrast is directly related to the number of electrons Z carried by each atom, thus distinguishing different atoms: the higher the number Z, the brighter the image.

High Resolution Transmission Electron Microscopy relies on viewing a very thin slice of the sample precisely parallel to columns of atoms in a chosen direction of the crystal structure. The transmission image shown in Fig. 1 is a view looking parallel to the plane of the CdSe/ ZnTe interface. In this projection of the structure, the images of the closest columns of metal and non-metal atoms are only partly resolved; they appear as a pair of unequal dots that blur into each other. But the dots can be clearly identified as two atoms with different values of their electron number Z. The respective brightness of the two dots is inverted on each side of an interface (A or B in Fig.1): In the image, one can differentiate high brightness/low brightness dots for CdSe (Z_{Cd}=48, Z_{Se}=34) and low brightness/high brightness dots for ZnTe layers (Z_{Zn}=30, Z_{Te}=52), see the insets at top of Fig. 1.

At the "ZnTe on CdSe" interface A, we see low brightness/ low brightness dots. Their quantitative intensity profile (Fig. 1) is consistent with Zn-Se bonds (Z_{Se}=34, Z_{Zn}=30). That is, the interface is a very thin slice of a third compound ZnSe, at the atomic scale (Fig. 2). This implies that, when the incident molecular beam is permuted from Cd+Se to Zn+Te during superlattice growth, the change in non-metal species (Te replacing Se) is retarded compared to the change in the metal species (Zn replacing Cd). The "CdSe on ZnTe" interface also appears to consist of a ZnSe-rich layer. High brightness/high brightness dot pairs never appear in the image of the superlattice, ruling out the presence of a CdTe interface layer.

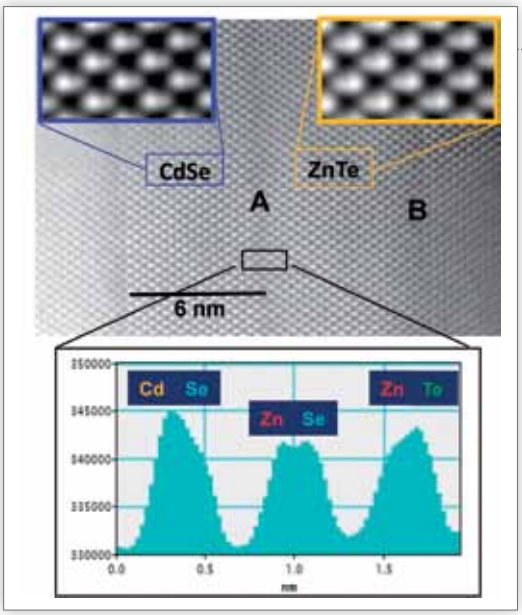

Fig. 1: *High resolution electron microscopy image of several layers of a CdSe/ZnTe superlattice. Growth direction is from left to right. Interfaces ZnTe-on-CdSe and CdSe-on-ZnTe are labelled A and B, respectively. Each bright spot represents a close pair of columns in the crystal structure (a column of metal atoms and a non-metal atom column).*

The two zooms show that the blurred bright "spots" consist of weak dot/bright dot pairs, corresponding to either (Cd, Se) or (Zn, Te) columns.

At bottom: *brightness profile across the interface A showing the Zn-Se bond nature of the interface.*

To add additional chemical insight to the image contrast analysis, the samples were investigated by Atom Probe Tomography (APT), another technique available at the Nano-Characterization Platform. A 3-Dimensional chemical mapping of atomic species can be done with (lower) spatial resolution by evaporating, atom by atom, a sharp tip fashioned in the material. $ZnSe^+$ molecular ions were detected, originating precisely from *all* the interfaces, but not CdTe molecular ions.

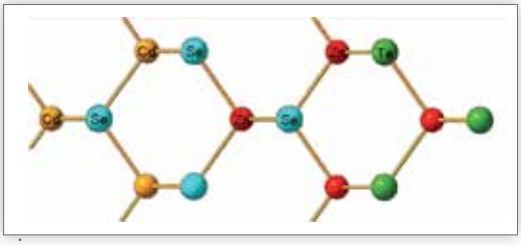

Fig. 2: *Atomic structure deduced for the interface between Cadmium Selenide (at left) and Zinc Telluride (at right), showing a Zn-Se bond at the interface. (Colour code: red=Zn, blue=Se, yellow=Cd, green=Te).*

The predominant formation of ZnSe bonds at both interfaces proves to be a very robust phenomenon: It persists under a wide range of crystal growth conditions investigated in this study. It is attributed to the difference in cohesive energies between the four possible metal/ non-metal couples, which clearly favours ZnSe.

CONTACT

Catherine BOUGEROL
catherine.bougerol@neel.cnrs.fr

Ph.D student:
Bastien BONEF

FURTHER READING

"Atomic arrangement at ZnTe/CdSe interfaces determined by high resolution scanning transmission electron microscopy and atom probe tomography"

B. Bonef, L. Gérard, J-L. Rouvière, A. Grenier, P-H. Jouneau, E. Bellet-Amalric, H. Mariette, R. André and C. Bougerol

App. Phys. Lett. **106**, 051904 (2015).

TeraHertz properties of multiferroic compounds

Electromagnetic waves outside the spectrum of visible light have been used for over a century to carry information (radio waves) or probe matter (X-Rays). However the spectral range known as the "TeraHertz gap" (Fig. 1) has hardly been explored because of a lack of good sources and detectors. Broadband spectroscopy at TeraHertz frequencies has now become available at synchrotron radiation sources. This spectral range is of considerable interest in Condensed Matter Physics, especially in magnetic or dielectric compounds, since both magnetic excitations (called magnons) and their electric analogue (optical phonons) have energies in this range. We have explored the TeraHertz response of compounds where new phenomena are expected, the so called "electro-magnons".

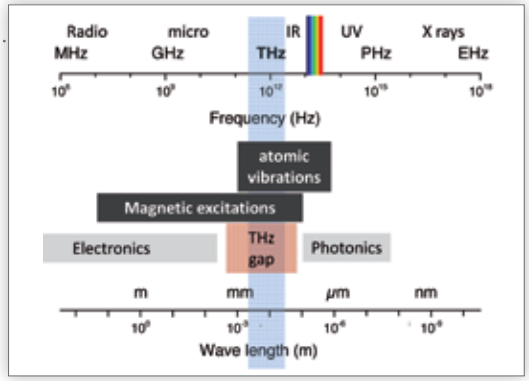

Fig. 1: *Electromagnetic spectrum from radio-waves to X-Rays. In the THz range, probed at SOLEIL and ILL, both atomic vibrations (phonons) and magnetic excitations (magnons and crystal-field excitations) can be studied.*

The manganite compounds of formula $RMnO_3$, where R is the transition element Y (Yttrium) or a rare earth element such as Dysprosium, Holmium, Erbium, are ferroelectric at room temperature: They show a spontaneous electric-charge ordering, giving an electric polarization directed along the principal axis (the c-axis) of the crystal's hexagonal lattice structure. These materials also present an antiferromagnetic order, typically below 80 K, associated with the Mn^{3+} ions (see Fig. 2). Compounds of this type, where both an electric and a magnetic ordering prevail simultaneously, are called "multiferroics". They are attracting considerable attention since they have potential applications for recording and manipulating information using both electric and magnetic fields.

We have focused on two members of this family, namely $YMnO_3$ and $ErMnO_3$. We have fully characterized their energy spectra in the TeraHertz (THz) range by combining two techniques available at large-scale facilities: THz spectroscopy at the synchrotron SOLEIL near Paris and inelastic neutron scattering at the Institut Laue-Langevin (ILL) in Grenoble. Both techniques allow measurements of the THz spectra, but bring different information.

Since the THz electromagnetic wave has perpendicular electric and magnetic field components, one can differentiate electric and magnetic excitations by their polarization dependence. That is, one can distinguish magnons, which are associated with the magnetic order and excited by the THz magnetic field, from optical phonons, associated with the ordered lattice of positive and negative ions and excited by the THz electric field. In $YMnO_3$, where the Y^{3+} ion is non magnetic, a sharp excitation is observed at 1.2 THz whenever the THz magnetic field is polarized perpendicular to the c-axis, for all orientations of the perpendicular electric field. It has all the characteristics of a magnon corresponding to the precession of the Mn magnetic moment around the c-axis. In $ErMnO_3$, where the rare earth ion Er^{3+} is magnetic, an excitation at the same energy is observed but polarization measurements show that it is excited only by the electric field, along the c-axis, not at all by the magnetic field!

One can also study THz excitations with neutron scattering. Since neutrons carry a magnetic moment, they can distinguish magnetic excitations from atomic excitations. Our neutron scattering measurements have confirmed the magnetic nature of the 1.2 THz (5.2 meV) excitation. These combined results demonstrate that a Manganese magnon has become electro-active in the Erbium compound. This is a new kind of excitation called an "electro-magnon". We attribute its electro-activity to the presence of the second magnetic ion in the material, the rare-earth Erbium, as follows.

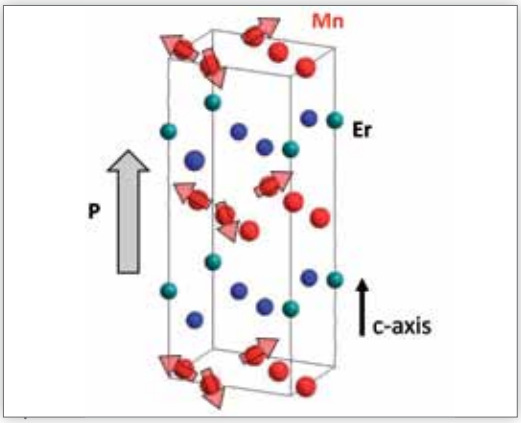

Fig. 2: *$ErMnO_3$ magnetic and electric orders. The electric polarisation is along the c-axis. The Mn magnetic moments are oriented at 120° from each other.*

It is known that the electronic levels in rare earth ions are shifted and split by the electrostatic field of the surrounding ions, the so-called "crystal field". Transitions between the crystal field-split levels may be allowed depending on the local symmetry. Thanks to our complementary probes, THz waves and neutrons, we have identified six such transitions for $ErMnO_3$. One of these transitions, at 2.1 THz, has the correct symmetry to be electro-active and to couple strongly to the magnon at 1.2 THz. The coupling interaction is then responsible for the complete loss of the magnetic character of the magnon: It has been transmuted into a purely electro-active excitation. This new mechanism for electro-magnons may be general to other rare-earth-based multiferroics and suggests new possibilities for manipulating these excitations through the action of magnetic and electric fields.

CONTACT

Sophie DE BRION
sophie.debrion@neel.cnrs.fr
Virginie SIMONET
virginie.simonet@neel.cnrs.fr

Ph.D student:
Laura CHAIX

FURTHER READING

"Magneto- to electroactive transmutation of spin waves in $ErMnO_3$"
L. Chaix, S. de Brion, S. Petit, R. Ballou, L.-P. Regnault, J. Ollivier, J.-B. Brubach, P. Roy, J. Debray, P. Lejay, A. Cano, E. Ressouche and V. Simonet
Phys. Rev. Lett. 112, 137201 (2014).

Implementing X-Ray diffraction/scattering tomography in the lab

Real materials often exhibit a complex and heterogeneous organization. Their distinctive functionalities are linked to their specific structure at the atomic scale as observed in alloys, cements but also in teeth, bones or archaeological materials. We have developed a method combining the diffraction and scattering of X-Rays with computed tomography. The diffraction/scattering information is used to detect, identify and image the various crystalline/amorphous phases in heterogeneous samples. This non-destructive analysis technique, first developed on synchrotron radiation facilities, can now be implemented at medium resolution on ordinary laboratory X-Ray diffraction equipment.

Tomography (from the Greek "tomos" = "slice") is a method for generating virtual images of slices through an object. In Diffraction and Scattering Computed Tomography (DSCT), the object is mounted in a very narrow beam of monochromatic X-Rays, and the diffraction and scattering intensities are recorded with a 2-Dimensional (*i.e.* multi-pixel) detector, see Fig 1. This is done with the object oriented at a large number N_ω of rotational positions ω, for each of a similarly large number N_y of horizontal positions *y*. From this very large mass of data, one can compute an image of the slice that contains structural information: chemical composition, atomic order (crystalline or amorphous, type of phase), grain size, etc. If desired, the object can then be translated vertically in steps to build a 3D representation as a stack of slices. DSCT also increases sensitivity to weak X-Ray signals coming from minor phases.

To implement DSCT in-laboratory, with spatial resolution ~200 microns, we adapted a multi-circle goniometer normally dedicated to single-crystal diffraction measurements and we added the translational and rotational stepping motions required for tomographic data acquisition. To acquire one slice, we record N_y x N_ω (N~100) diffraction images on a multipixel 2D detector. The various, randomly oriented, lattice-planes (*hkl*) in polycrystalline material diffract the incident X-Ray beam through their specific Bragg deviation angles 2Θ, giving the concentric rings in Fig. 1. Any highly disordered or amorphous materials scatter diffusely.

As illustration, we discuss our analysis of a carbon sample resulting from the phase transformation of Carbon 60 (C_{60} "fullerene" molecules) into a mixture of a crystalline rhombohedral polymer (C60R) and disordered graphite by high pressure (5 GPa) at 1100 K. Each of the N_y x N_ω 2D diffraction/scattering patterns is integrated azimuthally around its centre to convert it into a 1D pattern, *i.e.* diffraction/scattering intensity vs the deviation angle 2Θ, like that of Fig. 2a where we have labelled strong Bragg

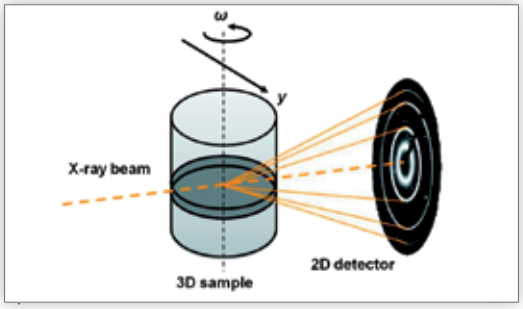

Fig. 1: *Geometry for X-Ray diffraction and scattering tomography analysis. To analyse one slice, the sample is translated in steps along y and rotated 180 deg. through angle ω.*

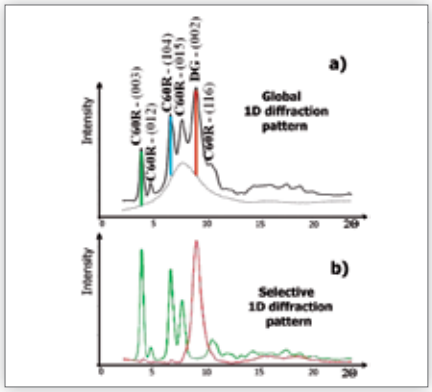

Fig. 2: (a) *A global 1D diffraction pattern for a slice through the transformed carbon sample shows Bragg diffraction peaks for lattice planes of its Rhombohedral C60 and disordered textured graphite (DG) components.*

(b) *Reverse analysis yields 1D-diffraction patterns selective for (in green) Rhombohedral C60 and (in red) disordered graphite.*

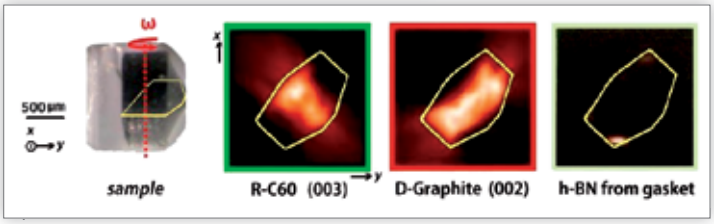

Fig. 3: At left: *The transformed carbon sample within its glass capillary container.*
At right: *Three phase-selective virtual slices as computed from the data for specific Bragg angles corresponding to (i) the (003) planes of the rhombohedral C60 component, (ii) the (002) planes of disordered textured graphite, and (iii) an unanticipated hexagonal-BN impurity. (The sample shape is outlined in yellow.)*

diffraction peaks for C60R and disordered graphite. From the complete set of N_y x N_ω 1D diffraction patterns, we can compute virtual slices that image the intensity scattered at a specific Bragg angle, versus *x* and *y* at height *z* in the sample. Additionally a reverse analysis of the transformed data can be performed in order to extract pure single-phase diffraction patterns (*e.g.* Fig. 2b) for all the phases within the heterogeneous sample, including unexpected components.

For our carbon sample (Fig. 3), we evidenced (i) rhombohedral C60 domains in the middle and lower part of the sample and (ii) disordered graphite domains in the external and top part of the sample. Interestingly (iii) a hexagonal Boron Nitride (h-BN) impurity phase coming from the high pressure gasket was also localized.

This work demonstrates that X-Ray diffraction/scattering tomography can be performed in the laboratory, with all the advantages of easy and instant access that this provides, even if the spatial resolution presently attainable (~100 microns) is very much lower than that obtainable at a Synchrotron radiation facility. Our technique will be particularly interesting for samples containing crystallites and/or heterogeneities a few hundred microns in size. It is suited for numerous practical applications like cements, alloys, catalysts, bones and paint cross-sections.

CONTACT

Olivier LEYNAUD
olivier.leynaud@neel.cnrs.fr

Pauline MARTINETTO
pauline.martinetto@neel.cnrs.fr

Ph.D students:
Michelle ÁLVAREZ-MURGA
Sophie CERSOY

FURTHER READING

S. Cersoy, O. Leynaud, M. Álvarez-Murga, P. Martinetto, P. Bordet, N. Boudet, E. Chalmin, G. Castets and J.-L. Hodeau
J. Appl. Cryst. 48, 159 (2015).

M. Álvarez-Murga, P. Bleuet and J.-L. Hodeau
J. Appl. Crystallogr. 45, 1109 (2012).

Strong roundceramic superconducting wires for very high field magnets

High magnetic fields have many advanced applications. In medical Magnetic Resonance Imaging they make it possible to scan the soft tissues of the human body, in Nuclear Magnetic Resonance spectroscopy, they enable studies of molecular structure and molecular interactions. Magnetic fields curve the paths of charged particles in circular particle accelerators like the Large Hadron Collider at CERN. They serve to confine the plasma in experimental thermonuclear reactors that produce energy by the same fusion reactions as occur in the sun. These and other applications are making continuing demands for more and more powerful magnets.

Very high magnetic fields can be produced by large electric currents circulating in a copper-wire magnet, but these currents dissipate energy by the Joule effect. The losses can be enormous. For example, at the Grenoble High Magnetic Field Laboratory, 24 MW are dissipated to produce a flux density of 36 Tesla in a 34 mm diameter bore. 24 MW is the average power consumption of a European town of 24 000 inhabitants! The solution for dramatically reducing the power consumption has been to use metallic superconductors, which have zero Joule losses below a critical temperature, T_c, near absolute zero. But the magnetic flux density is limited to a certain value, the "critical field" B_c, that destroys the superconductivity. Even the best metallic superconductors (niobium-titanium and niobium-tin alloys) cannot satisfy future needs for higher fields.

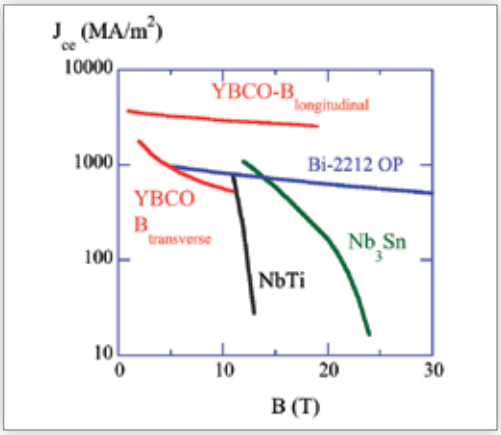

Fig. 1: *Engineering critical current density J_{ce} at liquid helium temperatures for superconducting wires used for winding high field magnets. (The "engineering" critical current density is the maximum sustainable current per unit area of the total cross-section of the wires, i.e. including non-superconducting structural and reinforcing materials.)*

Advances in High Temperature Superconductors are changing the situation. These ceramic materials, with values of T_c up to around 100 K, can outperform metallic superconductors when used at liquid Helium temperature. In particular, "YBCO" (Yttrium Barium Copper Oxide) and "Bismuth-2212" (Bismuth Strontium Calcium Copper Oxide, $Bi_2Sr_2CaCu_2O_x$) can remain superconducting up to very high current densities at 4 K, even under very high fields B, see Fig. 1.

YBCO can sustain very high currents, but has several drawbacks, notably its shape: it is supplied as very thin tapes. The Bi-2212 oxide can be produced as round wires, much better suited to building a magnet. And this compound has another big advantage: its absence of anisotropy. For YBCO, when the magnetic field direction is transverse (out of the plane of YBCO tape), the engineering critical current density J_{ce} decreases very rapidly (Fig. 1).

Recently the current carrying capacity of the Bi compound has been greatly enhanced using a new oxygenation process under high overpressure (D. C. Larbalestier *et al.*, *Nature Materials* 2014). Thus Bi-2212 round wire is now an attractive option for high field magnets. However its mechanical properties are not yet good enough to withstand the extremely high Lorentz forces experienced when it carries a high current under a strong magnetic flux density. An additional problem is that the oxygenation heat-treatment process for Bi-2212 must often be done after winding the wire into its final shape.

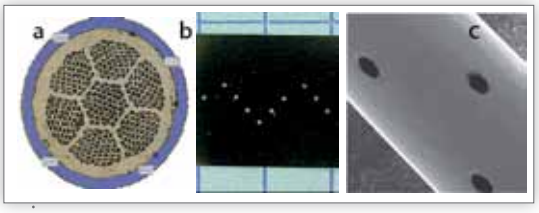

Fig. 2: ***(a)*** *Cross-section of a 0.8 mm diameter multi-filament Bi-2212 wire with our 50 µm thickness reinforcing sheath in Inconel (blue).* ***(b)*** *Inconel strip material with zigzag pattern of holes.* ***(c)*** *Tube-like sheath formed by rolling the Inconel strip round the wire and stretching it to fit; the holes (elongated by the stretching) enable oxidising heat treatment of the wire.*

In collaboration with the electrical-cable company Nexans-France, we have studied and implemented an original solution for mechanically reinforcing round Bi-2212 wires. The reinforcement is performed by a metal sheath wrapped around the wire using the Nexans company's shaping and welding process. This intricate and delicate process consists in mechanically shaping a thin strip of metal around the wire, then welding it by laser. Finally, the sheath is stretched to adjust to the wire diameter.

The 0.8 mm diameter Nexans Bi-2212 wire employed has seven sub-elements, each with 85 filaments of superconducting material, see Figure 2a. These filaments are embedded in a matrix of pure silver with a stronger alloy MgAg for the outer part. Several metals for the sheath were studied to determine their resistance to the heat treatment of the Bi-2212 and their mechanical properties after the treatment. We chose the austenitic, nickel-chromium based "superalloy" Inconel 601. It shows a good weldability, an acceptable ductility at room temperature, and it degrades the wire's critical current I_c only very slightly. To enable the oxygenation of the Bi-2212 during the heat-treatment, we developed a process of perforating the metal sheath in a "zig-zag" pattern (Fig. 2b and 2c) that minimizes weakening of the metal. The 50 µm thick external sheath increases the wire's mechanical stress resistance by a factor of 2.1 while reducing J_{ce} measured at 4 K by only 21%.

These results validate our reinforcement method, an essential step in making Bi-2212 wires a feasible solution for building big magnets for fields to 20 T and beyond.

CONTACT

Pascal TIXADOR
pascal.tixador@neel.cnrs.fr

FURTHER READING

"Mechanically reinforced Bi-2212 strand"

P. Tixador, C.E. Bruzek, B. Vincent, A. Malagoli, X. Chaud

IEEE Trans. Appl. Supercond. **25**, 6400404 (2015).

Metal colloids investigated by enhanced-Raman correlation spectroscopy

Metal colloids are suspensions of nanometre-size gold or silver particles dispersed in a liquid, here water. Under illumination by light, these solutions present unique and amazing optical properties that depend strongly on the size, shape and state of aggregation of the particles. However in spite of intense research work dedicated to metal colloids, understanding their optical properties in relation with the geometry of the particles as well as investigating their aggregation processes still poses a highly challenging task. Combining correlation analysis with Raman scattering measurements answers this challenge.

The rich optical properties of metal colloids are governed by the localized surface-plasmon modes of their constituent nanoparticles. These resonances are collective oscillations of the free electrons at the surface of the metal. They can be excited by light, which gives rise to resonantly-enhanced light absorption and emission properties as well as enhancement of the electric and magnetic fields at the nanoparticle surface.

Depending on various physical or chemical parameters (temperature, pH, adsorbed molecules...) nanoparticles may aggregate to form clusters ranging from simple dimers up to large and (more or less dense) fractal clusters composed of hundreds of particles. The electromagnetic interactions between the nanoparticles induce additional and stronger plasmon resonances than those of the individual particle, leading to possibly-total absorption of the incident light or to giant enhancements of the electromagnetic field in the nanoscale regions in between the particles.

These enhanced fields are in great part responsible for the so-called Surface-Enhanced Raman Scattering (SERS) effect, the enhancement by several orders of magnitude of the Raman scattering (*i.e.* the inelastic scattering of light) by molecules when they are adsorbed on the nanoparticles and trapped in such high field regions. As a consequence, metal colloids are currently used for ultra-sensitive detection of molecules, with wide applications in physics, chemistry, and biology. They are also very promising prospective candidates for in-vivo medical applications, such as intracellular imaging or in-body drug delivery, and are under investigation in the field of nanoscale thermally-activated processes such as nanocatalysis or photothermal therapy.

If the case of dimers is well understood, adding more nanoparticles rapidly increases the complexity of the system, hence posing a non-trivial task to relate their measured optical properties to those of an individual nanoparticle. There is consequently a need for in-situ characterizations of the aggregates and the aggregation processes, including the very first steps of the aggregation process.

To achieve this, we have developed an original experimental technique that associates correlation analysis with SERS spectroscopy (Fig. 1). A laser beam is tightly focused in the colloidal solution via a confocal microscope thus providing a very small observation volume. The laser beam excites the nanoparticles' plasmon-resonances responsible for enhancing the Raman scattering associated with excitations of the vibrations of the molecules adsorbed on these particles. We record the fluctuations of the Raman intensities as the particles diffuse in and out of the small observation volume, and we analyse these temporal fluctuations via auto-correlation functions (the correlations of the Raman signal with itself, at points separate in time), see Fig. 1. The correlation functions provide a characteristic time-value from which the nanoparticles' diffusion coefficient is inferred. Rotation of anisotropic clusters within the focus volume also provokes temporal fluctuations of the intensities, giving rise to a second characteristic time related to the rotational diffusion coefficient of the nanoparticles and/or clusters. From the values of the diffusion and rotation coefficients, and using hydrodynamic models, the size and shape of the nanoparticles/clusters can be identified.

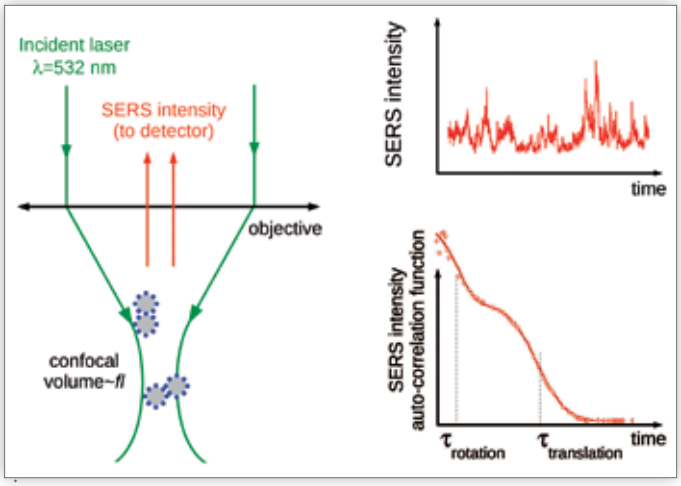

Fig. 1: At left: *A microscope illuminates a colloidal solution of nanoparticles (grey circles) carrying adsorbed molecules (blue dots). The Surface Enhanced Raman Scattering by the molecules, in the backwards direction, is recorded as a function of time* ***(top right)****. The auto-correlation function* ***(bottom right)*** *yields rotational and translational characteristic times related to the geometry of the diffusing objects.*

As a proof-of-principle we studied a model system of aggregates of ~30 nm diameter silver nanoparticles where the coagulation of the nanoparticles was induced by p-mercaptobenzoic acid (MBA) molecules. Depending on the MBA concentration, ranging from 1 to 10^{-3} millimoles/litre, different aggregation stages could be achieved and identified. For the highest concentration in MBA, we showed that large, isotropic clusters with an effective hydrodynamic radius almost 30 times larger than that of the isolated nanoparticle were formed. At lower MBA concentrations the first stages of the aggregation process could be studied. Dimers and chains of four nanoparticles were observed. Finally, in the case of the lowest MBA concentration, no aggregation occurred and the diffusion of the isolated nanoparticles of the initial colloidal solution was observed.

These results show that Surface-Enhanced Raman Scattering correlation spectroscopy is a very promising and powerful technique for in-situ studies of this kind. It enables the quantitative sizing and characterization of SERS-active aggregates and isolated nanoparticles. It thus paves the way to the practical task of in-situ monitoring of nanoparticle aggregation processes, in conjunction with basic research into the optical properties of the as-formed clusters.

CONTACT

Aude BARBARA
aude.barbara@neel.cnrs.fr

FURTHER READING

"SERS correlation spectroscopy of silver aggregates in colloidal suspension: quantitative sizing down to a single nanoparticle"
A. Barbara, F. Dubois, A. Ibanez, L. Eng and P. Quémerais
J. Phys. Chem. C 118, 17922 (2014).

"Non-resonant and non-enhanced raman correlation spectroscopy"
A. Barbara, F. Dubois, P. Quémerais and L. Eng
Opt. Exp. 21, 15418 (2013).

The PHYSIQUARIUM, a visitors' area at the Institut NÉEL

This dedicated visitors' area aims to make the story of scientific advances- past and present- comprehensible and attractive, and to provide glimpses of future developments. It was planned as a gateway to the Institut NÉEL's research work, adaptable for a varied public. It provides a pedagogical presentation of our work, including possibilities for simple demonstration experiments.

Fig. 1: *View of part of the visitor area.*

Opened in 2014, the PHYSIQUARIUM consists at present of three sections: Magnetism, Crystallography and Low Temperatures, three domains that are fundamental to much of the Institut NÉEL's research. Text, images and videos (accessed interactively via a touch-screen terminal), multiple posters and "hands-on" experiments introduce the visitor to the history of these three domains and present a selection of our recent discoveries and current work.

> *« Il est de notre responsabilité de vulgariser nos travaux pour les rendre accessibles à un plus grand nombre. »*
>
> Alain Schuhl, Director of the Institut NÉEL 2011-2014

Various frameworks for visits are possible. In 2015, these have benefited, in particular: classes from regional high schools; the winners of the national "Olympiades de Physique" competition; the general public during Grenoble's annual Fête de la Science; the undergraduate-level university students attending the International Nanosciences Summer School.

The first initiatives have interested some of the Institut NÉEL's partners. Representatives from Okayama University have visited the PHYSIQUARIUM to prepare the visit of 15 Japanese high school students in 2016. Locally, a formal collaboration has been started with our regional education authorities: a specific science-popularisation programme named "school@physiquarium". This programme is designed to actively engage high-school students, to stimulate their curiosity and sense of wonder, and to encourage them to apply all their powers of observation. Before the visits, the classes' science teachers meet with Institut NÉEL personnel and a supervising teacher for a day of preparation at the PHYSIQUARIUM. This enables the teachers to plan the most appropriate experiments to undertake with their students.

A specific programme also exists with the École des Pupilles de l'Air de Grenoble in which their post-baccalaureate year students develop new pedagogical experiments, for presentation at the PHYSIQUARIUM and possible integration into its panoply of experiments.

The researchers responsible for the PHYSIQUARIUM are Julien Delahaye, Jean-Louis Hodeau and Pierre Molho. Many Institut NÉEL staff and Ph.D. students contribute regularly to its success, including by welcoming the visiting students into their laboratories.

Popularisation of science is an important mission and the PHYSIQUARIUM is a concrete example of the Institut NÉEL's ongoing commitment to communicating with the public and especially to awakening young people to science. In return, our staff have been gratified by the response of teachers and their pupils. And for our Ph.D. students, the PHYSIQUARIUM provides an opportunity to present – often for the first time – their discipline to a non-specialist audience.

In 2016, a fourth section will be added to the PHYSIQUARIUM, called "Microscopies" (to include optical, electron, and near-field microscopies), which is another major area of the Institut NÉEL's research.

Fig. 2: *Observation.*

PHYSIQUARIUM
ESPACE VISITEUR DE L'INSTITUT NÉEL

CONTACT

Florence FERNANDEZ
florence.fernandez@neel.cnrs.fr

FURTHER READING

neel.cnrs.fr/physiquarium

Probing light fields with nano-mechanical oscillators

Because of their ultra-low mass, nanometre-scale objects can be used to measure applied forces with exceptional sensitivity, provided one can detect their vibrations. Here, a nanowire made of Silicon Carbide has been used to map the force field exerted by a focused laser beam. It is well known that the radiation pressure can have significant effects at the macroscopic and astronomical scales. What is radically new with nanowires is that we can study the mechanical action of light at a scale smaller than the optical wavelength. In addition, we can investigate the back action of the light on the nanowire's vibrational dynamics.

In collaboration with colleagues at the Institut Lumière Matière (Lyon) we have developed an experiment to probe the vibrations of nanoscale mechanical oscillators by an optical technique. Specifically, our nano-mechanical oscillators are crystalline Silicon Carbide nanowires having ultralow masses, of one-tenth of a picogram (10^{-16} kg). These oscillators are sensitive to forces in the attonewton range (10^{-18} N). They are one million times more sensitive than the (already very sensitive) probes used in the Atomic Force Microscopes that have been revolutionizing the nanosciences in recent years. We have used this extreme sensitivity to measure and map the mechanical action of light.

A 30 µm long, 150 nm diameter nanowire (Fig. 1a) was immersed in a laser beam that was tightly focused, down to a 500 nm spot size (Fig. 1b). First, by measuring the fluctuations of the light scattered by the nanowire, we characterized the nanowire's vibrations, whose fundamental eigenmodes have frequencies in the 10^2-10^3 kHz range. We were able to measure the thermal vibrational noise of the nanoresonator, (its "Brownian motion") over a very large dynamic range. This random motion determines the intrinsic force sensitivity of the nanowire, which amounts here to a few attonewtons at the temperature of the experiment, 300 K.

By moving the nanowire within the optical spot using a very precise piezo-electric positioning device, we then measured, in each point in space, the force exerted on the wire by the light field. Because the nanowire has such a tiny diameter, we could map the light-matter interaction with sub-wavelength spatial resolution (Fig. 1c). This represents a first step towards the investigation of vectorial force fields at the nanoscale, with unequalled sensitivity.

We also investigated how the presence of the optical force field can modify the nanowire's dynamics. This perturbation presents a fundamental character since it represents the return action or "back-action" of the optical measurement process, to which all measurement systems are intrinsically submitted.

In particular, we have investigated how the detailed shape of the vectorial force field (its "topology") was impacting the nanowire's dynamics. We have discovered a novel dynamical instability of the nanowire, leading to very large self-sustained oscillations, that appears in regions of strong vorticity of the light field. The existence of these regions is a consequence of the non-conservative character of the light-matter interaction. The regions of large shear can be directly visualized in the measured force-field's cartography (Fig. 1c), on each side of the optical axis.

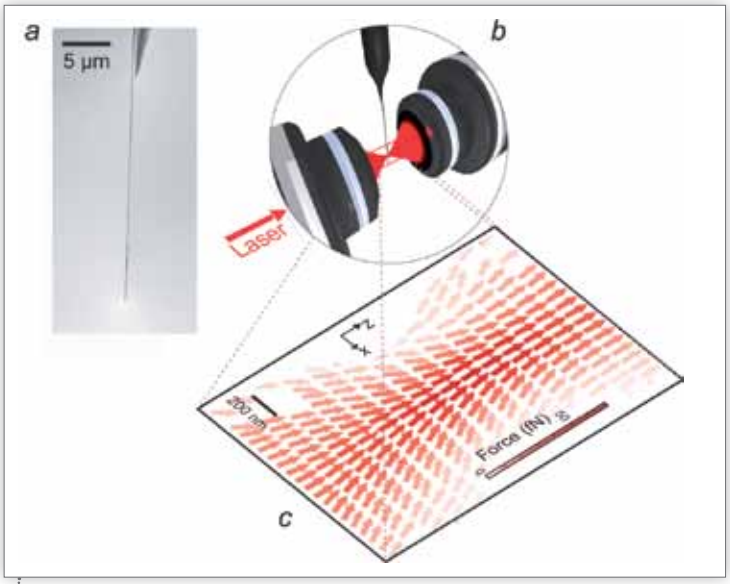

Fig. 1: (a) *Scanning Electron Microscope image of a 150 nm diameter Silicon Carbide nanowire, suspended at its top on a tungsten tip.*

(b) *The nanowire is piezo-positioned in a laser beam strongly focused by high numerical aperture microscope objectives. The nanowire's vibrations modulate the transmitted light beam intensity, which provides a means to characterize the nanowire's vibrations and measure its thermal noise.*

(c) *Due to a non-perfect cylindrical symmetry, each vibrational mode of the wire has two perpendicular components with slightly different frequencies. By amplitude-modulating the laser beam in resonance with these frequencies, the z and x components of the force exerted by the laser on the wire can be determined and mapped with large signal to noise (to give the field of red arrows). At high laser power, a dynamical instability is observed in regions of large shear in the vector flow, the irregularities seen here on each side of the optical axis.*

Often in physics, the dimensionality of the problem strongly affects the phenomenology observed. This is the case in this experiment, since the abovementioned dynamical instability cannot occur in the "mono-dimensional" optomechanical systems studied previously (resonators forming one end of a Fabry-Perot cavity) where the forces exerted by optical fields are conservative.

The optomechanical investigation developed in this work represents a new tool for investigating confined force fields. More generally, performing vectorial force field cartography provides a new analytical tool for investigating the light-matter interaction.

CONTACT

Olivier ARCIZET
olivier.arcizet@neel.cnrs.fr

Ph.D student:
Arnaud GLOPPE

FURTHER READING

"Nano-optomechanics and topological backaction in a non-conservative radiation force field"

A. Gloppe, P. Verlot, E. Dupont-Ferrier, A. Siria, P. Poncharal, G. Bachelier, P. Vincent, O. Arcizet

Nature Nanotechnology 9, 920 (2014).

Chiral domain walls in thin magnetic films

Magnetic domain walls are the transition regions between two magnetic domains with different magnetization directions. In ultra-thin films of a magnetic metal such as cobalt, having magnetization perpendicular to the film plane, the domain walls can be very narrow: 5 - 20 nm. Such domain walls can be moved at speeds faster than 400 m/s by in-plane current pulses and could be used as carriers of binary information in future high-density magnetic storage devices. These high speeds are possible because the magnetic configuration within the domain walls has definite "chirality": the magnetization rotates in the same direction in every wall in the cobalt layer.

The first observations of high-speed domain wall movement driven by an electrical current were made by Spintec Laboratory, Grenoble, in collaboration with the Institut NÉEL. This was in 0.6 nm (2 - 3 atomic layers) cobalt films sandwiched between a thicker layer of the non-magnetic metal platinum and an insulating layer of aluminium oxide (AlO_x). Following that discovery, it was proposed (Thiaville *et al.* EPL 2012) that two effects induced by the Pt/Co interface could explain such high propagation speeds.

First, the combination of a strong spin-orbit interaction in platinum and the breaking of the structural inversion symmetry by the interfaces can lead to a type of exchange interaction, called the Dzyaloshinskii-Moriya (DM) interaction, that favours a tilted alignment between neighbouring Co spins. This interaction can lead to domain walls where the magnetization rotates progressively in a plane perpendicular to the wall (see Fig. 1). This type of domain wall is well known (such walls are called Néel domain walls after Louis Néel) but in this system they have a special property: the sense of rotation is not random but is imposed by the sign of the DM exchange interaction, and is the same for all domain walls in the Co film. Hence the label "chiral domain walls".

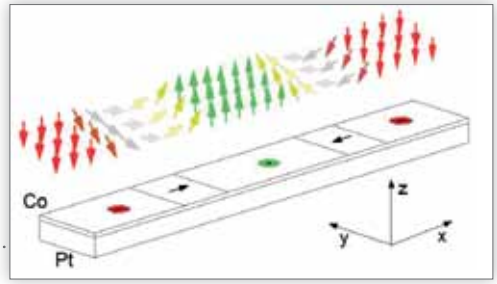

Fig. 1: *Two Néel domain walls with fixed left-handed chirality in a thin Co layer having perpendicular magnetization along z. The magnetization rotates to the left (anticlockwise around y) in both walls. Thus, the mean magnetization has opposite directions along x in the two successive domain walls.*

In this scenario, the second ingredient needed for efficient wall motion is a phenomenon called the Spin Hall effect that produces a spin-polarized electron current flowing from the Pt to the Co layer when an electrical current passes through the Pt layer. This spin current flow generates a strong torque that moves all the chiral walls *in the same direction* through the cobalt layer.

Fig. 1 illustrates the expected magnetization configuration of Néel walls with left-handed chirality. Notice in particular that the magnetization direction at the center of each domain wall is horizontal and opposite within the two, consecutive walls that separate down/up and up/down domains. We can make use of this property to prove that the domain walls are indeed chiral, by applying an in-plane magnetic field B_x: the energy of these walls will differ according to whether their mean magnetization is parallel or anti-parallel to B_x.

Fig. 2 shows images we have obtained using Kerr microscopy (magnetic microscopy with polarized light) for a rectangular Pt/Co/AlO_x microstructure. The magnetization of the cobalt is first saturated in the up direction. A magnetic field pulse is then applied in the down direction. With zero in-plane field (Fig. 2a), reversal of the cobalt's magnetization starts at a defect in the centre of the film. However, in the presence of an in-plane field B_x, nucleation starts either at the left edge (Fig. 2b) or at the right edge (Fig. 2c) of the structure, depending on the direction of B_x.

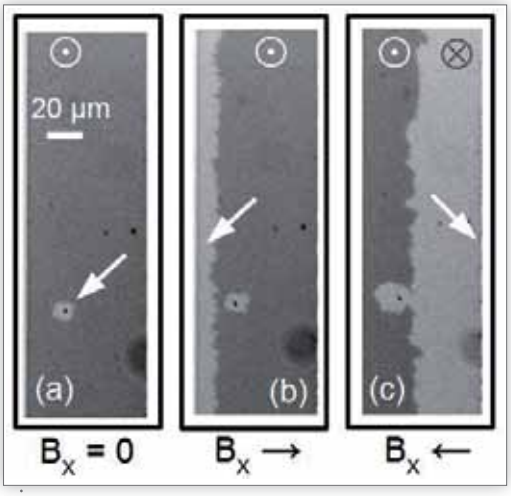

Fig. 2: *Kerr-microscopy demonstration of the left-handed chiral nature of Néel domain walls in a Pt/Co(0.6nm)/AlO_x microstructure. A small, perpendicular, magnetic field pulse B_z is applied in the down direction to a layer that had been initially magnetized in the up direction (dark grey). In* ***(a)****, with no in-plane field (B_x), a small domain with down magnetization (light grey) nucleates at a defect. With an in-plane field 260 mT directed right in* ***(b)****, or left in* ***(c)****, magnetization reversal starts along the left or right edge respectively, and spreads rapidly.*

These results confirm the presence of chiral Néel domain walls. By geometry, chiral walls created on the opposite edges have opposite in-plane magnetization (see Fig. 1). The nucleation takes place at the side where the domain wall's energy is lower, *i.e.* where its mean magnetization is parallel to B_x. A left-handed chirality (like in Fig. 1) can then be deduced from our measurements for the domains walls in the Pt/Co system.

The perpendicular field needed for nucleating an edge domain, *i.e.* to trigger reversal of the magnetization, depends strongly on the strength of B_x. By modelling this dependence we could obtain the strength of the Dzyaloshinskii-Moriya interaction in this system, which is $D = 2.2$ mJ/m^2. This is a high value and leads to a high stability of the domain walls in Pt/Co heterostructures, which is essential for high velocity propagation, making them a promising system for binary storage applications.

CONTACT

Stefania PIZZINI
stefania.pizzini@neel.cnrs.fr

FURTHER READING

"Chirality-induced asymmetric magnetic nucleation in Pt/Co/AlO_x ultrathin microstructures"

S. Pizzini, J. Vogel, S. Rohart, L. Buda-Prejbeanu, E. Jué, O. Boulle, I.M. Miron, C.K. Safeer, S. Auffret, G. Gaudin, A. Thiaville

Phys. Rev. Lett. 113, 047203 (2014).

Imaging inside Gallium Nitride wires for next generation blue LEDs

Semiconductors are both fascinating for physicists and extremely useful to society. The best-known semiconductor is Silicon, the material at the origin of the electronics and digital revolution of the second half of the 20th century. At the present time, the nitride materials Gallium Nitride (GaN) and its alloys are beginning another semiconductor revolution due to the specific properties of their energy bandgaps that enable them to emit visible light with unparalleled efficiency. The inventions at the origin of the nitride blue LEDs (Light Emitting Diodes) that are now penetrating the mass market for lighting applications were recognized by the 2014 Nobel Prize for Physics. We focus here on a potential next generation of these nitride LEDs, based on dense arrays of nitride microwires.

In the language of nano-technology, a "wire" is a very small crystalline object having length considerably greater than its diameter. Wire-based devices are a promising new route towards improved electronic and optoelectronic devices. Compared to present-generation nitride LEDs, which are conventional planar devices, wire devices have very desirable intrinsic properties such as small footprints and improved crystal quality. With careful design of donor and acceptor doping and alloy compositions, wires offer more versatility.

The building-block of optoelectronic applications is the p-n junction. In a LED, electrons from the n-type region and holes from the p-type region recombine at the junction, emitting light. Especially promising are p-n junctions in wires grown with the "core-shell" geometry: An n-type core (doped with the donor impurity silicon) is totally enclosed by a p-type shell (doped with the acceptor impurity magnesium). The shell is deposited on the lateral walls of the core and often also on the top of the core, see Fig. 1. Thus the p-n junction at the core-shell boundary has a three-dimensional (3D) character, very different

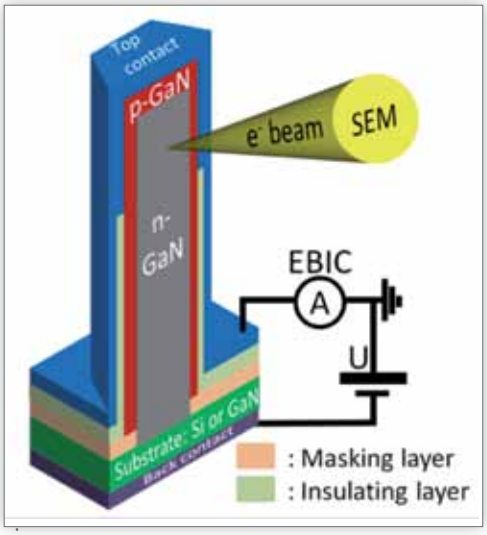

Fig. 1: *A cleaved, core-shell GaN wire, and its integration into a diode device for Electron-Beam Induced-Current (EBIC) measurements. The focussed electron beam creates electron-hole pairs or excitons in the GaN semiconductor; e-h pairs or excitons created in the p-n junction region are separated by the junction's electric field, and a net electric current flows through the device.*

from that of planar diodes. The wire's high ratio of surface to volume greatly increases the total area of the junction, and thus increases the proportion of active region in the device. This should alleviate the "efficiency droop" issue (a severe fall-off of efficiency at high current levels) in LEDs and will also be important for nitride-wire solar cells.

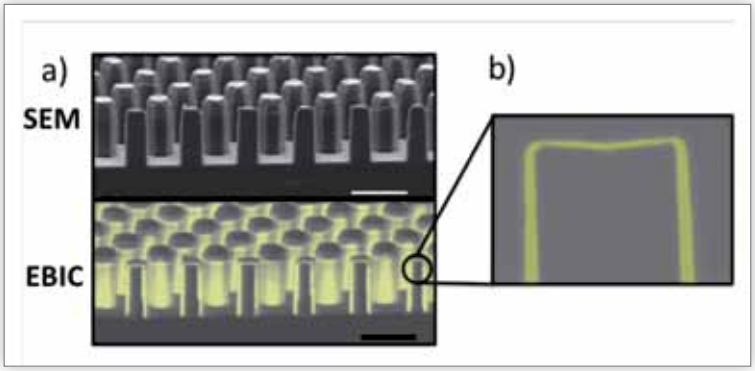

Fig. 2: ***(a)*** *Field Emission Scanning Electron Microscope (SEM) image at 10 keV for a processed, wire-based device, and the corresponding image (yellow colour) of the Electron Beam Induced Current intensity (scale bar: 10 µm). The wires in the front row were cleaved in half, so that the electron beam can probe inside them.*

(b) *A zoom onto the EBIC image shows lateral and top p-n junctions in a cleaved wire.*

Development of these nitride core-shell wire devices is hampered at present by a lack of precise knowledge about essential semiconductor properties along the buried 3D p-n junction. New, specific tools are needed to investigate the physical properties of the wire at the nanometric scale. We have now demonstrated how to image the electric field in a core-shell GaN wire and thus to determine the doping concentrations of the p-n junction.

Our diodes were wire arrays (Fig. 2) grown by the catalyst-free Metal-Organic Vapor-Phase Epitaxy technique on conducting GaN and Si substrates. The wires were grown and processed into device structures by colleagues at the CEA-LETI, Grenoble. To image the top and lateral junctions existing in the 3D diode structure, we exploited two powerful techniques available on a Scanning Electron Microscope, namely Electron-Beam Induced-Current (EBIC) and secondary-electron Voltage Contrast. We cleaved the substrates to split some of the GaN wires down their length (see Figs 1 and 2). With this cross-sectional approach and applying the scanning electron-beam techniques, we can achieve a spatially resolved analysis of the entire p-n junction, with nanoscale resolution.

The EBIC images (Fig. 2) enabled us to measure, at each point in the 3D junction, the diffusion lengths of current carriers generated by the electron beam (typically ≈60 nm on the p-type side of the junction and ≈15 nm on the n-side). The measurements also provided the width of the carrier depletion zone (40–50 nm). Under reverse bias of the diode, Voltage-Contrast Imaging provided electrostatic maps of the local electric potentials, from which we could deduce acceptor and donor impurity doping levels in the vicinity of the 3D junction (typically $N_a = 3 \times 10^{18}$ cm^{-3} and $N_d = 3.5 \times 10^{18}$ cm^{-3} in both the top and the lateral junction).

These nanoscale probing techniques provide values of the key parameters – carrier diffusion lengths, widths of space charge regions, doping levels – essential for guiding the further development of core-shell wire devices including LEDs and photovoltaic solar cells.

CONTACT

Fabrice DONATINI
fabrice.donatini@neel.cnrs.fr

Julien PERNOT
julien.pernot@neel.cnrs.fr

Ph.D student:
Pierre TCHOULFIAN

FURTHER READING

"Direct Imaging of p–n Junction in Core–Shell GaN Wires"

P. Tchoulfian, F. Donatini, F. Levy, A. Dussaigne, P. Ferret and J. Pernot

Nano Lett. 14, 3491 (2014).

Coherent control of a single nuclear spin with an electric field

Over the last four decades, the size of a bit, the smallest logical unit in a computer, has decreased by more than two orders of magnitude and will soon reach a limit where quantum phenomena become important. Inspired by the power of quantum mechanics, researchers have already identified pure quantum systems that have controllable and readable discrete states, in analogy with a classical bit. In this regard, the inherent spin of an atomic nucleus with its two (or more) eigenstates is a promising candidate. We have developed a molecular transistor which allows us to write quantum information onto a single nuclear spin purely by means of an electric field, as well as to do an electronic read-out of the quantum state. This novel approach opens a path to addressing and manipulating individual nuclear spins, that is to handle information localized in a very small space (a single atom), at high speed.

The magnetic moment of a nuclear spin is ten billion times smaller than the magnetic moment of one bit of a modern hard drive. To succeed in detecting such a tiny signal, we first developed a very sensitive magnetic field sensor – the Single-Molecule Magnet (SMM) spin-transistor (Fig. 1). The heart of this device is a single metalorganic molecule. It is a terbium "double-decker" single-molecule magnet, which works as amplifier and detector for the terbium ion's nuclear spin.

To amplify the nuclear spin signal, we make use of the "hyperfine" interaction between the terbium's nuclear spin and its electronic spin. By mapping the nuclear spin state onto the terbium's electronic spin state we amplify the magnetic signal by a factor of 10000. In a second stage of amplification we read-out the nuclear spin dependent magnetic moment of the terbium ion via the tunnel current through the molecular transistor. This is possible as the terbium's electronic spin interacts strongly with the tunnelling electrons via its exchange coupling with those electrons.

In recent experiments at very low temperature (30 mK), we were able to show that the terbium's nuclear spin can be manipulated purely by an oscillating electric field (the microwave field represented in Fig. 1). This is remarkable because the magnetic dipole associated with the nuclear spin is, to first order, by its very nature, sensitive to magnetic fields only.

Our experiment is explained by the hyperfine Stark effect, which acts as a magnetic field transducer at the atomic level. When we apply an electric field, it modifies the electronic wave functions of the terbium ion (a "Stark Effect"). This modification in turn changes the coupling of the electronic and nuclear spins, the "hyperfine interaction". The altered hyperfine interaction is seen by the nucleus as a change of the effective magnetic field at the nucleus. Therefore an oscillating electric field is transformed into an oscillating effective magnetic field. If the frequency of this oscillation is brought into resonance with the spacing between the nuclear spin levels, a coherent manipulation of the nuclear spin states is possible. Furthermore, the hyperfine Stark effect also allows us to shift the resonance frequency of our nuclear quantum bit ("qubit") by means of a *static* electric field, which can be easily generated by applying a back-gate voltage.

The use of oscillating electric fields to manipulate nuclear spins could facilitate the integration of multiple spin-qubits in a device architecture, since electric fields are much easier to focus and to shield than magnetic fields. Moreover, the use of a static back-gate voltage to tune individual nuclear spin qubits in and out of resonance provides a possibility for addressing individual qubits using only a single-frequency microwave signal. Thus, single-molecule magnets are promising candidates for quantum information processing, and could lead to the appearance of a new field of research: molecular quantum electronics.

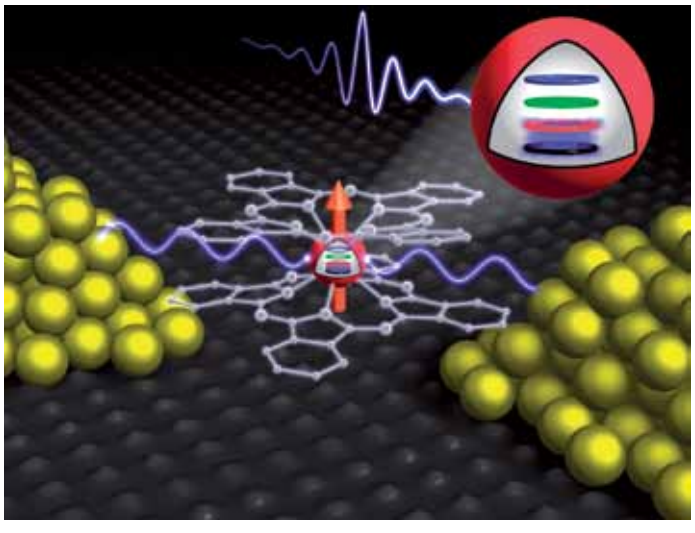

Fig. 1: *The single-molecule magnet spin-transistor. The heart of the device is the terbium "double-decker" single-molecule magnet: two planar organic molecules enclosing a Terbium ion. The "magnet" is connected to two metallic leads (gold atoms) deposited on a substrate. We apply a voltage across the two contacts to establish a tunnelling current through the molecule. The read-out of the (I=3/2) ^{159}Tb nucleus's four spin states (depicted in the enlargement as coloured rings) makes use of a change in this tunnelling current that occurs at well defined values of an applied external magnetic field. At these field values, the nuclear spin state is resonant with the microwave electric field pulse (blue wave).*

CONTACT

Franck BALESTRO
franck.balestro@neel.cnrs.fr

Wolfgang WERNSDORFER
wolfgang.wernsdorfer@neel.cnrs.fr

Ph.D student:
Stefan THIELE

FURTHER READING

"Electrically driven nuclear spin resonance in single-molecule magnets"

S. Thiele, F. Balestro, R. Ballou, S. Klyatskaya, M. Ruben, W. Wernsdorfer

Science 344, 1135 (2014).

Resistivity, magnetism and shape memory in martensitic alloys

The martensitic phase transformation plays an important role in transformations of the microstructure and plasticity of many materials. The term martensite referred originally to a structural phase of carbon steel alloys named after German metallurgist A. Martens. This term has gradually been extended to other metallic alloys possessing a first order, solid to solid, phase transition of "displacive" nature (that is one where all the atoms shift slightly, all together at the same time, without any long-range diffusion of the alloy's different atoms). The resulting lattice deformation leads to a new crystal structure with new properties. Certain ferromagnetic alloys of nickel, manganese and a third element such as gallium constitute a particularly interesting case. Under application of magnetic field or pressure, they exhibit large changes of electrical resistivity, entropy or magnetization, and even an astonishing ability to change shape reversibly. These are properties which have promising industrial applications in actuators, current limiters, switches, refrigerators.

The alloys of interest here are the so-called "Heusler" alloys of formula Ni_2MnX (where element X = Ga, In, Sn, Sb…). The parent phase of the martensitic transition is "austenite" (another name from steel-making history). Because of the symmetry-lowering during the structural phase transition, the nucleation of the martensite phases within a crystal of the austenite phase, induced by cooling, allows multiple structural configurations with different orientations that are called "variants".

Due to its displacive nature, the transformation proceeds by cooperative movements of the atoms, keeping the same atomic order as the austenite parent phase. The nucleation of a single martensite variant within an austenite crystal would require an enormous elastic energy. This energy is greatly reduced when there is an additional lattice invariant shear to the homogeneous lattice deformation occuring by "slip" or "twinning". A modulated martensite structure usually appears and consists of building blocks of the structure twinned in a way to compensate for the difference in the martensite and austenite lattice constants. A thermal hysteresis consequently appears, because there is a frictional barrier opposing the interfacial motion of the nucleating phase.

A subtle balance between the structural and magnetic states resulting from the off-stoichiometry (deviations with respect to the precise base-formula Ni_2MnX) allows a wide range of multi-functional properties. When pressure or a magnetic field is applied, a large strain or a change in shape (of up to 10% in Ni-Mn-Ga alloys) can be induced via a structural reorientation of the martensite variants by twin-boundary motions. The variant selection depends on its shear strain or its magnetic moment with respect to the applied stress or magnetic field. The original shape can be recovered by heating above the structural transition temperature (the "shape-memory" effect).

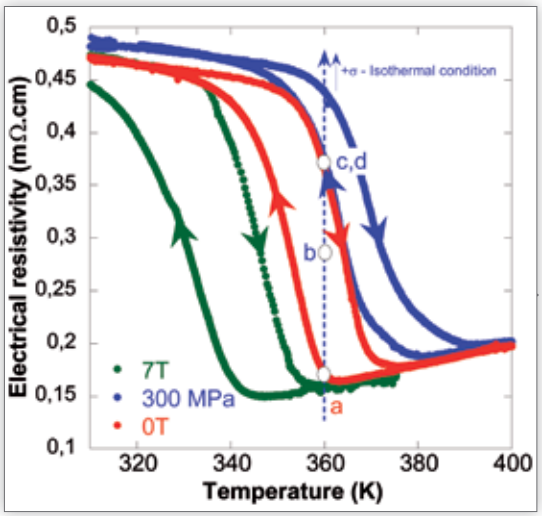

Another very interesting property is the shift of the martensitic transformation temperature on application of pressure or a magnetic field, see Fig. 1, which shows resistivity data for the case of a Ni-Mn-In alloy with some Cobalt. The transition is shifted towards higher temperature under pressure and towards lower temperature under magnetic field. Thus, at fixed temperature, large magnetoresistance effects, or piezoresistance effects (*e.g.* the vertical line in Fig. 1) of up to several hundred %, are observed.

These effects are the direct consequence of the possibility to transform the austenite phase into a martensite phase by applying a pressure, and to transform martensite into austenite by applying a magnetic field.

The process can be fully reversible, or irreversible (see Fig. 2), depending on whether the external field is applied during the heating or the cooling branch of the hysteresis. There is thus a large range of possibilities for coupling the different functional properties of these materials for application to new sensors, switches, actuators, and other devices.

Fig. 1: *Three hysteresis loops for the resistivity of a $Ni_{45}Co_5Mn_{37.5}In_{12.5}$ single crystal as it is temperature-cycled through the transition from austenite (at high T) to martensite (at low T). The red loop is for zero field, zero pressure. Applying a magnetic field (green loop) shifts the transition temperature down, applying pressure (blue loop) shifts it up. At fixed temperature (360 K), the material can be transformed through different states a, b,.. by varying the pressure.*

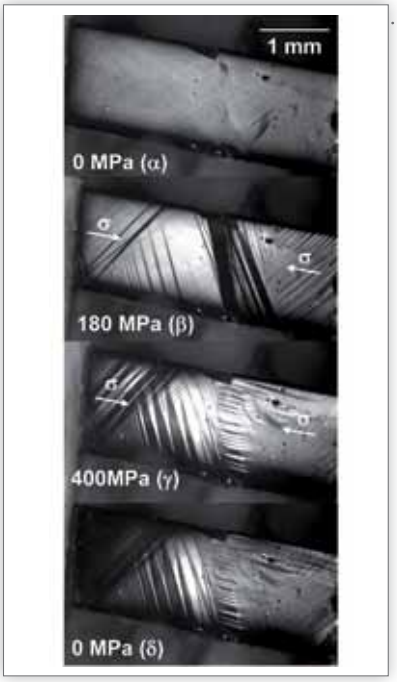

Fig. 2: *Optical microscope images of a single crystal of NiMnIn alloy under increase and release of pressure, showing irreversibility of the transformation of the crystal's microstructure if pressure is applied and released at a cooling point in the hysteresis cycle. Arrows σ show the applied uniaxial stress direction (squeezing direction).*

CONTACT

Daniel BOURGAULT
daniel.bourgault@neel.cnrs.fr
Laureline PORCAR
laureline.porcar@neel.cnrs.fr

FURTHER READING

"Large piezoresistance and magnetoresistance effects on $Ni_{45}Co_5Mn3_{7.5}In_{12.5}$ single crystal"
L. Porcar, D. Bourgault and P. Courtois
Appl. Phys. Lett. 100, 152405 (2012).

"Irreversibility of the martensitic transformation in Ni-Mn-In single crystal studied by resistivity under pressure and in situ optical observations"
L. Porcar, P. Courtois, G. Crouigneau, J. Debray and D. Bourgault
Appl. Phys. Lett. 105, 151907 (2014).

Synchrotron X-Ray study of platinum-nanoparticle catalysts

Better knowledge of metal nanoclusters supported on an oxide is of paramount fundamental and technological importance especially in the field of energy. In particular, dispersed platinum particles on alumina (aluminium oxide Al_2O_3) are widely used as heterogeneous catalysts, from the laboratory scale to the industrial plant. A specific case is catalytic "reforming" where petroleum refinery naphtas (liquid hydrocarbon mixtures) are converted into high-octane products. The catalyst's reactivity and selectivity are intimately related to the local geometry and the electronic density of the active sites. They strongly depend on the coverage with hydrogen, often present in the reactive medium, and on the alumina support. It is now possible to characterize such systems at the atomic level, and *in situ*, that is at a temperature and hydrogen pressure close to the catalytic process conditions. X-Ray Absorption Near Edge Spectroscopy (XANES) is one of the few techniques allowing such a study in disordered materials.

The XANES experiments were performed at the European Synchrotron Radiation Facility, Grenoble, on a system containing 0.3 weight % Pt supported on 10 nanometer width alumina platelets. The platelets have mainly (110) and (100) faces for 70% and 20% of the exposed surface, respectively. The platinum is in the form of a cluster of atoms of size smaller than 1 nm. We choose Pt_{13} particles to model the clusters in an appropriate way. A comparison between data from the XANES experiments and modelling enables us to obtain the atomic positions within the clusters and the hydrogen coverage, as well as providing information about the sites and faces of the supporting material on which the nanoparticles are adsorbed. Note also that, in the experiment, hydroxyl (OH) groups remain present on the alumina (110) face and some dispersion in the nanoparticle size was observed by Scanning Tunnel Microscopy.

The number of parameters involved, and the lack of reference X-Ray spectra to compare with, makes simulations mandatory to gain quantified insights from the experimental data. Recording the spectra using the High Energy-Resolution Fluorescence-Detection mode is also necessary. The spectra were obtained in the energy region of the Pt-L_3 X-Ray absorption edge where the X-Ray photoelectric process generates a transition from a core 2p level of the Pt atom up to the Pt metal 5d valence band states. Experiments were realized at two temperatures, 25°C and 500°C, and two values of hydrogen pressure, 10^{-5} and 1 bar. The higher temperature is typical of operating conditions in catalytic reforming.

The quantitative assignment is then done in two steps: First, a set of structural models is provided by the Density Functional Theory - Molecular Dynamics (DFT-MD) approach. This is done for the 2 alumina faces, including effects of the reconstruction of the alumina surface induced by the Pt cluster itself and the different possible hydrogen coverages. Secondly, using these models, we perform *ab initio* simulations of the XANES spectra, based on the full multiple scattering theory, and compare them to the data.

We found that the sensitivity of the calculated spectra to the geometrical models is high. In Fig. 1, we show only the final result, with the best agreement we got, for two operating conditions. In this way, we obtain the corresponding solutions for the hydrogen coverage and the cluster structure at the two main faces. For example, at 25°C and 1 bar, models containing 18 and 20 hydrogen atoms give the best fit to the spectra. We also found from the calculations that, whatever the H-coverage, the clusters on the (100) face remain bi-planar whereas they have a 3D morphology on the (110) face, although strongly distorted compared with the original cluster calculated without hydrogen. On the (110) face, the hydroxyl groups reduce the negative charge of the metallic clusters and therefore the number of electrons available for hydrogen adsorption. Consequently at low pressure, we find more hydrogen atoms on clusters on the other face. In contrast, in the experiment performed at 25°C and 1 bar, the cluster morphology on the (110) face is changed into a distorted cuboctahedron, with fewer direct Pt-alumina bonds, leaving more adsorption sites available for hydrogen atoms.

Thus, high resolution XANES analysis, *in situ* under hydrogen reaction conditions, coupled to DFT-MD calculations, have allowed us to discriminate the different morphologies of supported nanoparticles and to quantify hydrogen coverage. This detailed understanding of highly dispersed platinum particles should help to achieve better control of catalysts under reductive environment. This work also brings new methodologies for the interpretation of XANES analysis, used in the characterization of many systems.

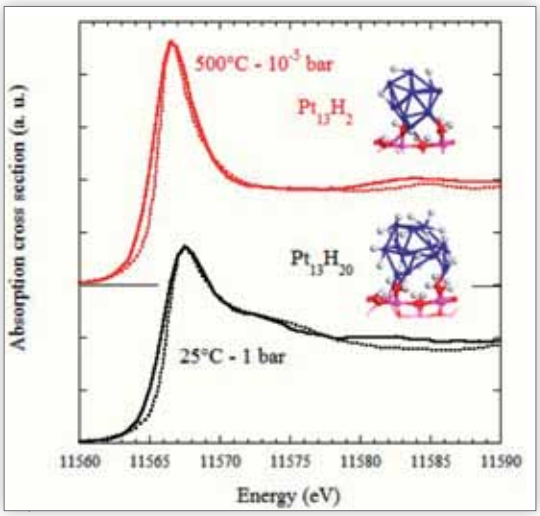

Fig. 1: *Sensitivity of the XANES spectra, at the Pt-L3 X-Ray absorption edge, to the morphology and hydrogen coverage of platinum clusters on alumina. Simulated spectra (solid line) are compared with the data (dashed line) recorded under two different temperatures and hydrogen gas pressures. The models shown are the best models for the clusters on the Al_20_3 110 face under these operating conditions. Colour code: blue= Pt, grey = H, purple = Al, red = Oxygen.*

CONTACT

Yves JOLY
yves.joly@neel.cnrs.fr

Ph.D student:
Agnès GORCZYCA

FURTHER READING

"Monitoring Morphology and Hydrogen Coverage of Nanometric Pt/gamma-Al_2O_3 Particles by In Situ HERFD–XANES and Quantum Simulations"
A. Gorczyca, V. Moizan, C. Chizallet, O. Proux, W. Del Net, E. Lahera, J-L. Hazemann, P. Raybaud and Y. Joly
Angew. Chem. Int. Edition 53, 12426 (2014).

Multifunctional substrate holder for a film-deposition system

Many of the Institut NÉEL's research projects require constructing specialist equipment in-laboratory, to precise specifications. We describe here a technical development that has greatly improved a system used for high-rate deposition of thick magnetic films onto silicon substrates by DC sputtering. These films are studied for their functional magnetic properties and their integration into novel microsystems.

In Direct Current (DC) sputtering (*pulvérisation*), a "target" material, made from a metal or metallic alloy, is bombarded by charged plasma ions (*e.g.* Ar^+). This bombardment ejects metal atoms from the target, which then deposit on a substrate positioned nearby. We have designed and built a greatly improved substrate holder (Fig. 1) for an existing sputtering system, to enhance possibilities for growth and integration of functional magnetic films.

The specifications: A first requirement was to heat 4 inch (10 cm) diameter silicon substrates *uniformly* over their entire surface, up to temperatures of 800 °C in vacuum or under low pressures of argon or nitrogen. A second requirement was to be able to rapidly cool the substrate from high temperature, at the end of film growth or post-deposition annealing. This is in order to control the film's microstructure (grain size, etc.) and to manage mechanical strain. Also, the distance between the substrate and the target must be adjustable, and the substrate must be rotatable during deposition to achieve homogeneous composition and thickness. Finally it should be possible to bias the substrate at up to -300 Volts (2 Amps current) to enable film etching, which required adding baffles to prevent stray deposition producing short circuits between parts at -300 V and grounded parts.

Our greatest constraint was to fit this new, relatively large substrate holder in the limited space of an existing growth chamber yet be able to rotate it within the chamber to achieve three working positions (90 degrees apart) for substrate loading, film deposition, and annealing, respectively. To respect all these specifications, we had to overcome many technical challenges.

The heater component: The substrate support (Fig. 2) is made from a block of the Molybdenum alloy "TZM" (Mo with 0.5% Titanium and 0.08% Zirconium), a material that represents a good compromise as concerns mechanical resistance at high temperature, thermal conductivity, re-crystallization temperature and evaporation under vacuum.

The 240 V, 8 A heating element was made from tungsten wire. We shaped the wire into the form of a coiled spring at 300 °C, where tungsten becomes ductile. The coil was then inserted into sections of alumina tubes for insulation. Alumina (Al_2O_3) is compatible with tungsten up to 1900 °C, has excellent electrical insulating and heat conducting properties, and its relatively high emissivity optimizes radiative heat transfer to the TZM block. This heating element is mounted inside the TZM block (see Fig. 2). Extensive testing was done to determine the best operating temperature of the wire for safe, prolonged operation (1500° C) and the optimum length of wire (15 m) to match the power supply's impedance at this temperature.

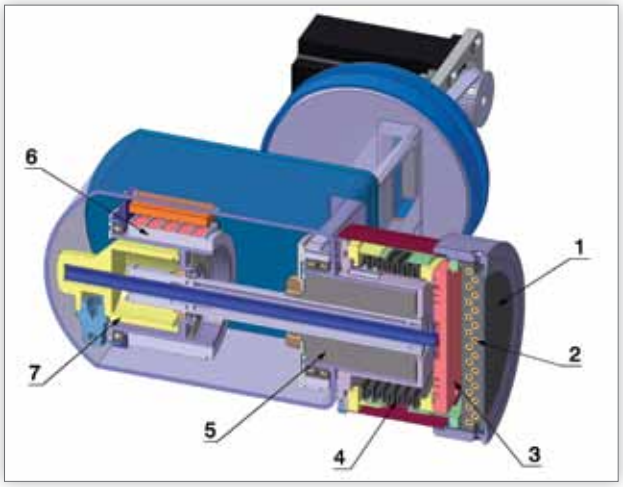

The fast cooling system: This is based on the original idea of using a copper "flange and bellows" unit filled with cold water. To cool the TZM block rapidly, the water pressure is increased to expand the bellows (*soufflet*), thus bringing the flange (*bride*) into sudden contact with the TZM block.

We chose a bellows made up of four concentric thin walls, which increases the deformability and reliability of the bellows, while keeping it rigid enough not to stretch during evacuation of the chamber. The water circulating in the bellows also serves to screen the radiation coming from the hot TZM block, thus protecting vulnerable parts such as the electrical connections and the magnetic ferrofluidic joint which seals the rotation-axis.

The upper face of the TZM block was honed to a matte surface to increase its heat radiation to the attached substrate. The opposite face, which comes into contact with the copper cooling flange, was highly polished to achieve maximum planarity and a bright surface to limit downward radiation. *An important detail:* We milled the copper flange under pressure to compensate for deformation of its surface at working pressure. Thus it is perfectly flat when the pressure forces it into contact with the TZM block (otherwise, only the centre would be in contact).

The improved sputtering system is being used for studying a range of functional magnetic materials (hard, soft, magneto-caloric) in the framework of both EU and industrial projects.

Fig. 1: *Section drawing of the substrate holder. During film deposition, a 4 inch diameter silicon substrate is attached to the outer surface of the molybdenum alloy block, at the right of the image.*

1: *Molybdenum alloy block.*

2: *Heating element.*

3: *Copper flange.*

4: *Bellows.*

5: *Ferrofluidic vacuum rotary feedthrough.*

6: *Slip-rings for power, thermocouple and bias voltage.*

7: *Water-supply rotary swivel.*

Fig. 2: *The molybdenum alloy block, seen upside down, with the tungsten coil heating element visible through the holes. The highly polished under surface minimizes heat radiation into vulnerable elements underneath it. The substrates are attached to the top surface (the opposite surface, not seen in this photo).*

CONTACT

Richard HAETTEL
richard.haettel@neel.cnrs.fr

Creation and manipulation of magnetic monopoles in spin ice

Condensed matter near the absolute zero of temperature reveals much exotic physics associated with unusual orders and excitations, with examples ranging from helium superfluidity to magnetic monopoles in the solid materials called "spin ices". The far-from-equilibrium physics of such low temperature states may be even more exotic, yet to access it in the laboratory remains a challenge. We have demonstrated a simple and robust technique, that we call the "magnetothermal avalanche quench", that can be used in the controlled creation of non equilibrium populations of magnetic monopoles in spin ice at millikelvin temperatures.

In 1931, Dirac asserted that if just one magnetic monopole exists, then charge (both electric and magnetic) must be quantized. This was based on a hypothetical conjecture that stretching a magnetic dipole by taking one of the poles out to infinity, would leave behind a magnetic charge, attached to an imaginary string of dipoles for the return flux. Although a "Dirac monopole" has not yet been observed, its classical analogue is believed to occur in certain magnetic systems, the rare earth oxides with the pyrochlore crystal structure, $Dy_2Ti_2O_7$ and $Ho_2Ti_2O_7$ (Dysprosium Titanate and Holmium Titanate).

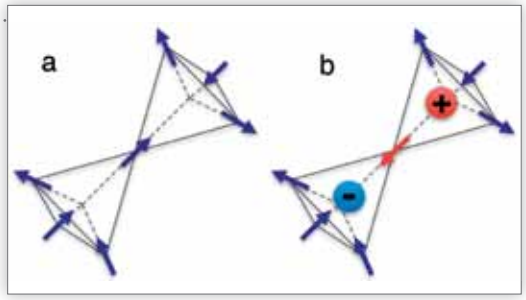

Fig. 1: ***(a)*** *Two corner-sharing tetrahedra of rare earth spins in a pyrochore crystal structure, each obeying the ice rule "two spins point in, two spins point out".*

(b) *Departures from the ice rule create effective magnetic monopoles. The monopoles may occur in adjacent tetrahedra as shown here, or separated.*

These compounds are said to be geometrically "frustrated": They show no magnetic order because the magnetic interactions cannot all be satisfied simultaneously. The magnetic ions in these compounds (the rare earth ions) form a network of corner-sharing tetrahedra, and have a strong magnetic anisotropy: Their magnetic moments align along a <111> axis (a diagonal) of their local tetrahedron. This combined with dipole-dipole interaction gives rise to the "ice rules" (so-called by analogy with the rules for the O-H bonds in water ice). Simply stated, the minimum energy state corresponds to two rare earth spins pointing in and two spins pointing out of each tetrahedron (Fig. 1a).

This 'ice-rule' is equivalent to a divergence-free condition on the total magnetic moment on each tetrahedron, and thus, in analogy with electromagnetism, can be viewed as a vacuum of magnetic charges. In this picture, thermally activated defects, *i.e* three spins in and one out (or vice versa) on a given tetrahedron (Fig. 1b), create a magnetic charge on that tetrahedron, and correspond to an effective magnetic monopole. That is, in the vicinity of the defect, the magnetic field looks like the field of a monopole. The density of these monopoles in zero applied field goes to zero with temperature. Nevertheless it has been shown theoretically that a fast thermal quench could create long-lasting monopole-rich states at low temperature.

In recent measurements of the magnetic moment of $Dy_2Ti_2O_7$ at temperatures <1 K, we have demonstrated the importance of the quench rate on the dynamic properties. In addition, we proposed a new protocol, which we call the magneto-thermal avalanche quench technique, that results in a density of effective monopoles more than an order of magnitude greater than the one generated by the fastest conventional cooling experiments in zero field.

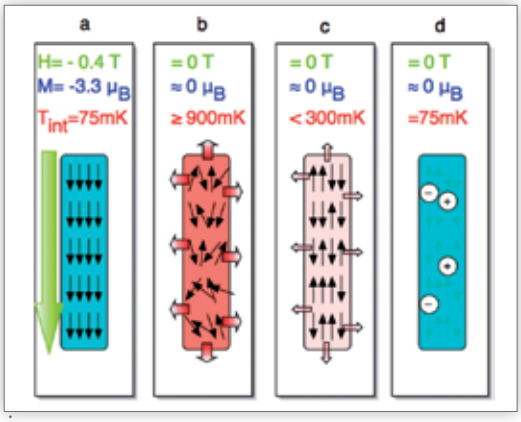

Fig. 2: *The avalanche quench technique. Each tetrahedron has been replaced by an arrow that represents the direction of just one of its apex spins.* ***(a)*** *The magnetism of the sample is first saturated in a high field at low temperature* ***(b)*** *the field is switched off, which heats the sample,* ***(c)*** *the heat is evacuated leaving* ***(d)*** *a large density of defects (monopoles). Signs + and - represent effective magnetic monopoles.*

The trick is to exploit the heat that is created by the magnetic work done on the sample when the field is rapidly changed, which will cause a sudden increase in temperature solely inside the sample. The sample then finds itself at relatively high temperature but connected to the cold thermal bath. The ensuing quench is the most efficient and rapid possible. Our avalanche technique is illustrated in Fig. 2. The sample's magnetization is first saturated in a field of 0.4 Tesla and cooled to 75 mK. Then the field is rapidly switched off and the magnetic Zeeman energy $\Delta M \cdot H$ released (from the spins flipping back towards spin-ice configurations) heats the interior of the sample to approximately 900 mK. This heat evacuates to the still very cold mixing chamber of the helium dilution refrigerator. The sample cools extremely fast, limited only by the thermal conduction to the copper sample holder. The result of the avalanche quench is to freeze-in a very large, non-equilibrium density of monopoles.

In subsequent experiments, we have shown that applying a magnetic field to this non-equilibrium state produces a magnetic current, *i.e.* a current of monopole charges, analogous to an electric-field driven current of + and - electric charges in an electrolyte. Our technique thus opens a path for studies of the intrinsic far-from-equilibrium dynamics of spin ices at low *T*, which is dominated by magnetic monopoles.

CONTACT

Elsa LHOTEL
elsa.lhotel@neel.cnrs.fr

Carley PAULSEN
carley.paulsen@neel.cnrs.fr

FURTHER READING

"Far-from-equilibrium monopole dynamics in spin ice"

C. Paulsen, M. J. Jackson, E. Lhotel, B. Canals, D. Prabhakaran, K. Matsuhira, S. R. Giblin and S. T. Bramwell

Nature Phys. 10, 135 (2014) ; also see "News & Views" by H.-B. Braun, *Nature Phys.* 10, 88 (2014)

Long-distance entanglement between spins in quantum spin chains

The macroscopic world surrounding us is much more complex than it was thought by the greatest scientists of the 19th century and before. After the mathematical completion of the most significant theory of the 20th century, quantum mechanics, it became clear that new concepts had to be incorporated, although they may defy common sense and human perception may have difficulty accepting such strange predictions. This is the concept called "entanglement".

Take two photons, A and B, issued from the *same* process and send them to opposite places. Both photons are part of the same state and cannot be described independently, no matter how far apart in space and time they are. They are said to be entangled. Therefore, if the polarization of photon A is changed, photon B will sense this change instantaneously. New areas of research are being developed where entanglement could be at the origin of the interactions in ever larger objects, ranging from photons to clusters of atoms to molecules (and even to cosmological objects).

A very fruitful area of research today is applications of entanglement in quantum computation and quantum communications. For short-range or mid-range communication, it has been proposed to use spin chains as quantum channels. Among many possible spin configurations, certain antiferromagnetic spin arrays can exhibit true entanglement of pairs of spins. In the language of magnetism, entanglement is akin to spin dimerization, S= 1/2 spins coupled in pairs, having a singlet ground state S=0. The entangled photons A and B are now the discrete pairs of coupled spins A and B present in certain antiferromagnetically coupled spin systems.

There are many examples of compounds displaying this interesting physics. In particular, low dimensional systems incorporating chains or ladders of spin-pairs have been widely studied. Unfortunately the spin-dimerization (or entanglement) in the low-dimensional compounds studied so far takes place between adjacent spins, so these compounds are not interesting for long-distance quantum information transport.

For the first time we have demonstrated experimentally that two S=1/2 spins separated by some tens of nanometres can entangle via an intervening set of spin singlets (Fig. 1) in a bulk material, the strontium-copper oxide $Sr_{14}Cu_{24}O_{41}$. This compound has a complex crystal and magnetic structure. There is a stacking of two parallel antiferromagnetic sublattices, a spin chain and a spin ladder, both lattices having an overall spin-singlet ground state S=0. Along the chain and ladder direction (the c-axis direction), the two sublattices are arranged in a "misfit structure" with a non-rational ratio of their respective lattice parameters: c_{chain}/c_{ladder} ~10/7.

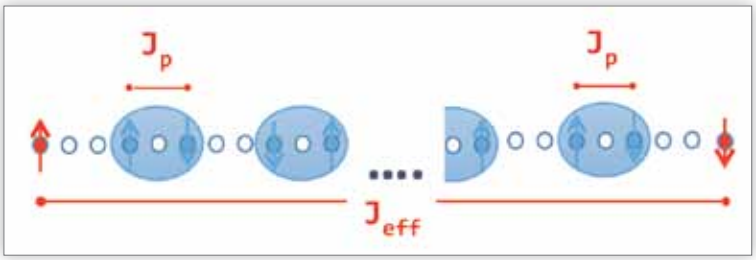

Fig. 1: *A chain of spin dimers (in blue) separated by magnetically inactive lattice sites (white dots) in the compound $Sr_{14}Cu_{24}O_{41}$. The spins (arrows) are magnetic copper ions. The dimers are characterized by a relatively strong spin-exchange interaction $J_p \approx 115K$. The dimer chain connects two isolated S=1/2 spins (in red) separated by a distance of order 10 nm. The effective spin exchange, J_{eff}, coupling ("entangling") these isolated S=1/2 spins is of order a few Kelvin.*

Our low-temperature magnetization measurements (*e.g.* Fig. 2) and specific heat studies as a function of magnetic field reveal the presence of very dilute, very weakly coupled spin dimers S=0 in this cuprate crystal, as illustrated in Fig. 1. The dimers are evidenced by their very small spin gap to very low lying excited triplet states S=1, confirmed by the observation of the quantum phase transitions (*i.e.* transitions driven not by temperature but by a magnetic field) related to the field-induced splitting of these excited triplets. The mechanism producing the isolated S=1/2 spins of Fig. 1 is the modulation of the interaction potentials between the two misfitting sublattices.

The results of this work are conceptually important as they indicate how, by controlling the periodicity of an inter-sublattice modulation, one could produce unpaired spins located at a given and controlled distance in a quantum spin 1/2 chain, for studies of quantum information transport.

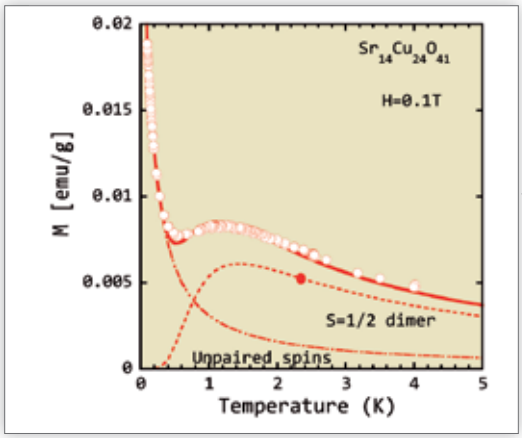

Fig. 2: *Magnetization as a function of temperature below 5 K (open red dots). The relative maximum at 1.3 K is interpreted as arising from the presence of spin dimerization between distant unpaired spins with a singlet-to-triplet gap of Δ_1 ~2.3 K (filled red dot). The rapid rise below 1 K is attributed to a small concentration of unpaired spins that remain uncoupled down to our lowest temperature. Dashed and dash-dotted lines are the fit with the corresponding equations.*

CONTACT

José-Emilio LORENZO-DIAZ
jose-emilio.lorenzo-diaz@neel.cnrs.fr

FURTHER READING

"Experimental realization of long-distance entanglement between spins in antiferro-magnetic quantum spin chains"
S. Sahling, G. Remenyi, C. Paulsen, P. Monceau, V. Saligrama, C. Marin, A. Revcolevschi, L. P. Regnault, S. Raymond and J. E. Lorenzo
Nature Physics 11, 255-260 (2015).

2D nanoporous graphene: a route to organic topological insulators?

The electronic and structural properties of a system are tightly connected and by experimenting with structure researchers are able to play with quantum electronic properties. Ultimately-thin materials like graphene (a single plane of carbon atoms) provide numerous illustrations of properties dominated by low-dimensionality. These properties can be enriched by engineering more advanced structures, where a "superpotential" imposed on the honeycomb lattice of graphene opens electronic band-gaps or creates new electronic bands. In particular, certain graphene-like honeycomb structures, exhibiting atomically well-defined pores regularly spaced by nanometre distances have been predicted to be two-dimensional topological insulators, *i.e.* materials that are insulators except at their edges, where the electronic structure leads to one-way conduction channels.

The family of known 2D topological insulators is restricted to only a few systems (HgTe/CdTe and InAs/GaSb heterostructures, Bismuth bilayers). A strong enough spin-orbit coupling, as conferred by the presence of high-atomic number elements, is required to open up a bandgap throughout the interior of the 2D system. The prospect for applications based on topological insulators, in the fields of spintronics, micro-electronics, metrology, and thermoelectricity, raises the key questions of their cost of production and their eco-friendliness. With these constraints in mind, our aim was to realize a 2D *organic* topological insulator based on a graphene nanoporous network.

For this purpose we used an approach exploiting molecules as building blocks (designed by F. Chérioux and co-workers at the Institut FEMTO-ST in Besançon), assembled into nanoporous networks through chemical reactions mediated by metal surfaces. Such surface-mediated chemistry is a rapidly developing field of research where only a few reaction schemes have been proposed and tested. Fig. 1 shows a Scanning Tunnelling Microscopy (STM) image of the product of a surface reaction which we have discovered: a reaction between $CO(CH_3)$ acetyl groups leaving only water as a by-product. The product is a fully covalent, atomically-thin, carbon-rich network on a metal surface, whose degree of order is currently being optimized.

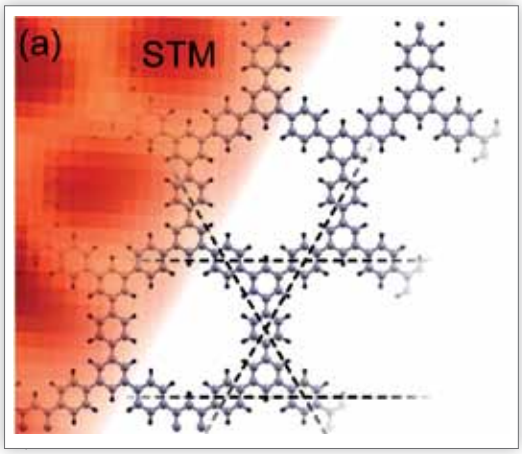

Fig. 1: *At top left, a Scanning Tunnelling Microscope image of a nanoporous network grown on a gold substrate. The superimposed schema at bottom-right shows the interpretation of this image: a hexagonal symmetry 2- Dimensional network of chains of benzene rings enclosing large "pores".*

Density functional theory (DFT) calculations were run to support the STM data and to reveal fine details of the structure that are not accessible with the spatial resolution of the STM. Also, DFT highlights the very peculiar electronic band structure of this 2D system. It shows a large band gap (larger than 2.5 eV) and a valence band characteristic of a so-called Kagome lattice – a lattice paved by hexagons each surrounded by six up – and down-pointing triangles. The calculations found one flat band, and two bands crossing at the corner of the Brillouin zone (point K in Fig. 2) with linear dispersion in the vicinity of the crossing point.

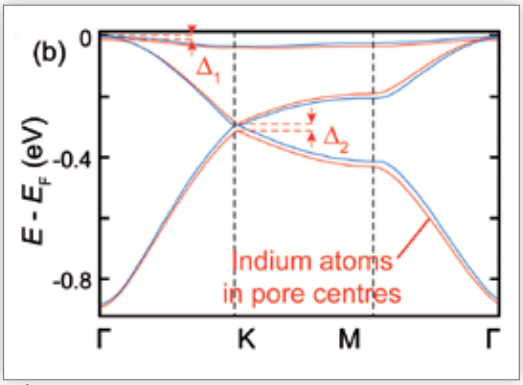

Fig. 2: *Zoom onto the valence band of the calculated band structure (electron energy vs k-vector). The blue curves are for a nanoporous network as grown in this work. Note the band degeneracies at Brouillon zone critical points K and Γ. The red curves show how placing a heavy atom (Indium, having strong spin-orbit coupling) in the pores of the lattice could remove these degeneracies (giving splittings Δ_1, Δ_2), thus producing a topological insulator.*

We also calculated the effect that adsorption, onto the lattice, of a heavy atom (Indium) with large spin-orbit coupling could have. It would open small gaps at the two degeneracy points (Γ and K in Fig. 2) turning the ideal system into an insulator. Analysis of the wave-function shows that the system indeed has non-trivial electronic properties typical of a topological insulator.

Future experimental and theoretical work will address networks formed from molecular precursors enclosing high atomic number elements which are expected to enhance the effect of spin-orbit coupling.

CONTACT

Johan CORAUX
johan.coraux@neel.cnrs.fr

Laurence MAGAUD
laurence.magaud@neel.cnrs.fr

FURTHER READING

"Convergent fabrication of a nanoporous two-dimensional carbon network from an aldol condensation on metal surfaces"

J. Landers, F. Chérioux, M. De Santis, N. Bendiab, S. Lamare, L. Magaud and J. Coraux

2D Materials 1, 034005 (2014).

9

neel.cnrs.fr

Highlights 2015

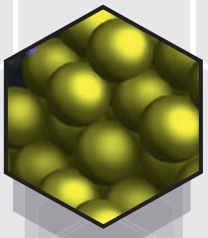

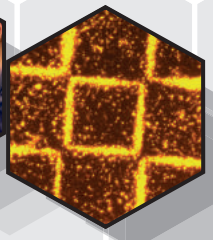

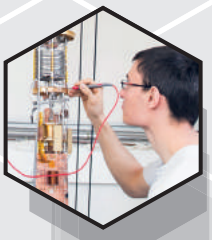

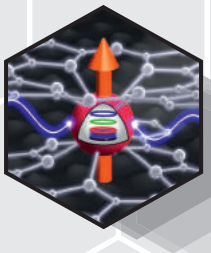

Institut NÉEL
25, rue des Martyrs
B.P. 166
38042 Grenoble Cedex 9, France
neel.cnrs.fr

Crédit photos : Institut NEEL - Visuel couverture : SYNTHESE-ECA - Tél. : 04 79 90 02 73